

Size-Frequency Distributions Of Rocks Around Impact Craters In The InSight Landing Ellipse In Elysium Planitia, Mars. K. R. Devlin^{1,2}, N. R. Williams¹, M. P. Golombek¹, I. J. Daubar¹, A. Huertas¹, M. R. Trautman¹, R. B. Hausmann^{1,3}. ¹Jet Propulsion Laboratory, California Institute of Technology, Pasadena, CA 91109; ²Temple University, Philadelphia, PA 19122; ³Oregon State University, Corvallis, OR 97331.

Introduction: The InSight (Interior Exploration using Seismic Investigations, Geodesy, and Heat Transport) mission landed on November 26, 2018, in Elysium Planitia on Mars [1-2]. Its landing site is a Hesperian lava flow degraded by impacts and aeolian processes, and images taken by InSight show numerous rocks ejected and emplaced by impacts [3]. The distribution of rocks around craters is not uniform; proximal ejecta tends to contain larger and more abundant rocks versus distal ejecta [4]. In this study, we examine the spatial distribution of rocky ejecta surrounding impact craters across the landing ellipse to provide a broader context for the rocks in view of the lander.

Data and Methods: During landing site selection, hazards including rock abundance were investigated and mapped throughout the final landing ellipse [5]. Rocks were identified using a supervised semi-automated detection algorithm [6, 7] to find individual rocks based on their shadows in HiRISE (High Resolution Imaging Science Experiment) images at a resolution of around

0.25 m/pixel [8]. We mosaicked 75 available HiRISE images covering the InSight landing ellipse and compiled rock lists from 64 of those images that contained detectable rocks. We visually inspected the entire ellipse to select 400 impact craters with a significant number of rocks in their ejecta (Fig. 1). For each crater, we plotted the relationship between boulder size and distance from the crater center for all rocks located between 1 and 5 crater radii (Fig. 2). Only rocks >1.5 m in diameter are reliably detected and measured in HiRISE images, so measured rocks were fit to exponential models to derive the cumulative fractional area (CFA) of all rocks [6]. We evaluated the total CFA in radial bins with 0.25 radii increments between 1 and 5 radii to assess the radial distribution. We modelled CFA around an impact crater using the power law $CFA(\%) = k \cdot r^{-1/\tau}$, with r as the radius of the crater, k is the CFA at the crater rim, and τ describes the radial distribution of the rocks [9]. We created plots to investigate the range and radial trends of CFA (Figs. 2-3).

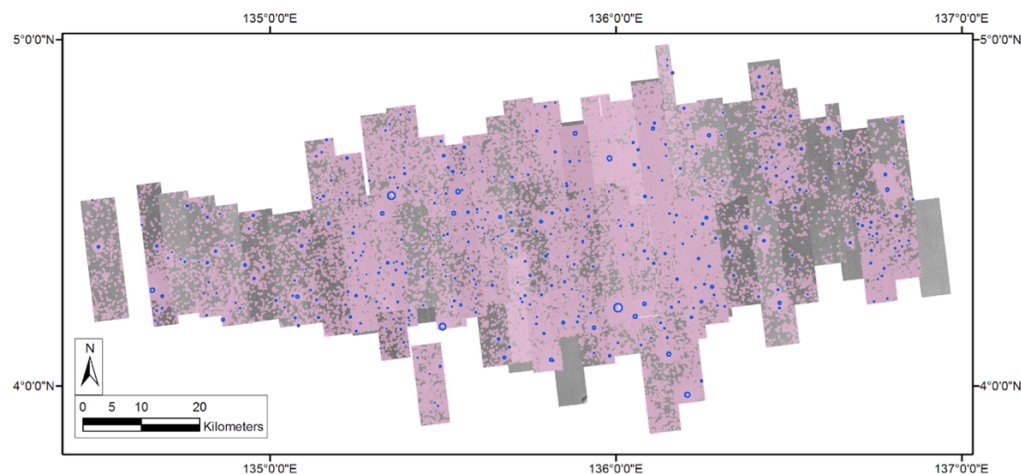


Fig. 1: Locations of all 921,142 detected rocks within the landing ellipse (pink) and the 400 craters selected with high rock abundances in their ejecta (blue).

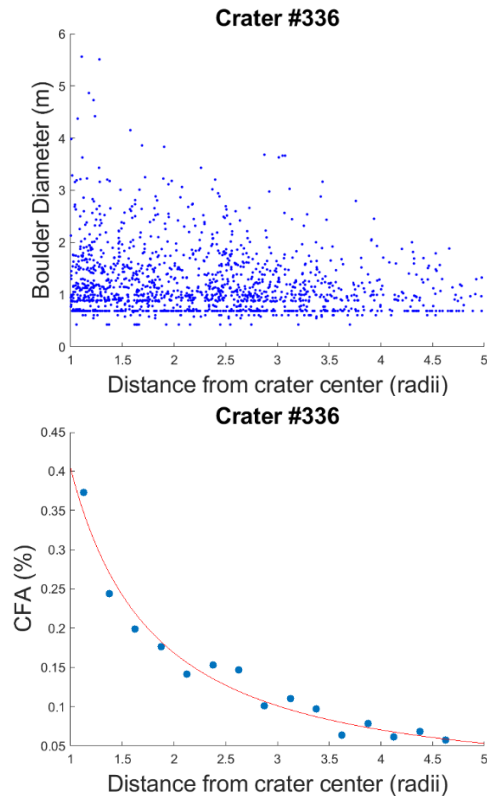


Fig. 2: Example radial rock distribution around a crater showing a generally decreasing trend between boulder diameter and distance from crater center (top), and its associated binned CFA and power law fit (bottom).

Results: The list of all rocks measured consists of 921,142 individual rocks, of which 458,368 are between 1 and 5 crater radii from the selected crater centers. Rocks around these craters all exhibit generally decreasing trends of maximum boulder diameters with increasing distance from crater centers (Fig. 2). Radially binned CFA also consistently decreases with increased radial distance, following an inverse power law. The coefficients k and τ for CFA fits for all selected craters show an inverse trend with high k values occurring at low τ values and low k values at high τ values (Fig. 3). R^2 values indicating variance and showing the goodness of fit for each crater are also highest for relatively high values of k , especially when $k > 0.2$.

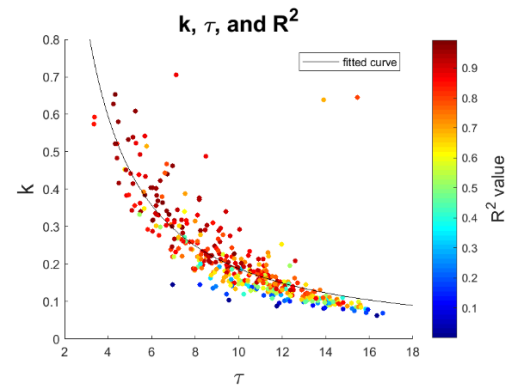


Fig. 3: Coefficients to radial CFA distribution for all examined craters, with a power law fit to illustrate the trend. Dot colors represent the confidence (R^2 value/variance) for each crater.

Discussion: Over all selected craters, k and τ are inversely related with very few outliers. This indicates that craters with the most rocks around them also have the strongest radial decrease. R^2 values are typically above 0.7 for the rockiest craters ($k > 0.2$), adding confidence to the CFA model. The trend in k and τ values does not correlate with crater size over the range examined, although smaller craters may not excavate all the way through the regolith to bedrock and thus have an abnormally lower k independent of τ [3]. Younger craters have less time for degradational processes to take effect and thus should have more rocky ejecta remaining and exposed than older craters [11]. We predict that higher values of k coupled with lower values of τ may be used to quantitatively provide constraints to relative crater age and degradation state [3,10,11].

References:

- [1] Golombek, M. P., *et al.* (2019) 50th LPSC, this issue. [2] Parker, T. J., *et al.* (2019) 50th LPSC, this issue. [3] Warner, N. H., *et al.* (2019) 50th LPSC, this issue. [4] Bart, G. D., and Melosh, H. J. (2010) *Icarus* 209, 337-357. [5] Golombek, M. P., *et al.* (2017) *Space Sci. Rev.* 211, 5-95. [6] Golombek, M. P., *et al.* *JGR* 114, (2009). [7] Golombek, M. P., *et al.* *JGR* 108, (2003). [8] McEwen, A. S., *et al.* (2007) *JGR* 112, E5. [9] Williams, N. R., *et al.* LPSC 49 Abs. 2819, (2018). [10] Warner, N. H., *et al.* (2017) *Space Sci. Rev.* 211, 147-190. [11] Sweeney, J., *et al.* (2018) *JGR*, 123, 2732-2759.